Research article

Journal of Human, Health and Halal Metrics; 2020, 1(2): 47-55
https://doi.org/10.30502/JHHHM.2021.249912.1025

Fabrication and characterization of chitosan-polyvinyl alcohol-graphene oxide nanocomposite scaffold for wound healing purposes

Fariba Saeedi[1], Arash Montazeri[1*], Yaser Bahari[1], Malihe Pishvaei[2], Behrooz Jannat[3], Mahdi Rasa[4], Fatemeh Saeedi[1]

1- *Department of Nanotechnology, Faculty of Engineering, University of Guilan, Rasht, Iran.*
2- *Institute of Color Science and Technology, Tehran, Iran.*
3- *Halal Research Center of IRI, Ministry of Health and Medical Education, Tehran, Iran.*
4- *Department of Biology, Faculty of Sciences, University of Guilan, Rasht, Iran.*

Submission: 24 September 2020 ***Revision***: 10 November 2020 ***Acceptance***: 5 January 2021

Abstract

Background and objective: Traditional transplant methods have been replaced by tissue engineering as a novel treatment. It involves the use of nanocomposite scaffolds with or without cells. Bacterial infection is one of interfering factors against suitable wound healing because it poses the site at risk of long-term side effects. Protection of wound from bacteria is necessary for its better recovery. Selection of appropriate materials for wound dressing is facilitated by understanding of wound healing mechanism and the compounds' properties. Our study aimed to evaluate biological characteristics of chitosan (CS)-polyvinyl alcohol (PVA) (50:50) scaffold reinforced with graphene oxide (GO) for wound healing.

Materials and methods: For fabrication of nanocomposites, ultrasound waves helped in better distribution of GO within the polymer matrix and scaffolds were prepared by casting method. The nanocomposite scaffolds were characterized by fourier transform infrared spectroscopy (FTIR), X-ray diffractometer (XRD), and scanning electron microscopy (SEM) to find out dispersion of GO in the polymer matrix. Biological characteristics were examined by *in vitro* antibacterial tests.

Results and conclusion: The scaffold reinforced with 3% (w/w) GO showed better morphological and biological properties than the others. Suitability of the scaffolds for cell proliferation was confirmed by MTT (3-(4,5-dimethylthiazol-2-yl)-2,5-diphenyltetrazolium bromide) cell toxicity test. Absorption (λ = 570 nm) of CS-PVA (50:50)/3% (w/w) GO scaffold increased by 84% compared to CS-PVA (50:50) scaffold. Inhibition zone of CS-PVA (50:50)/3% (w/w) GO was 18 and 20 mm for *Pseudomonas aeruginosa* and *Micrococcus luteus*, respectively, that was higher than the inhibition zone measured for CS-PVA (50:50) scaffold. According to cell viability result, mouse fibroblast cells (L929) could adhere on the CS-PVA (50:50)/3% (w/w) GO nanocomposite scaffold. In conclusion, GO could improve the biological properties of CS-PVA (50:50) scaffold so that the complex would be appropriate for wound healing.

Keywords: Chitosan, graphene oxide, nanocomposite, polyvinyl alcohol, wound healing

*Correspondence to: Arash Montazeri; e-mail: A.montazeri@guilan.ac.ir; Tel.:+98-1333690274; Fax:+98-1333690270

1. Introduction

Polymers are used as scaffold in tissue engineering for adhesion and differentiation of cells without delay [1]. Tissue engineering technology includes repairment of the damaged organs by self-regeneration of the cells in the presence of biomolecules and mechanically supporting structures. This technology restores memory of the damaged tissues to their earlier times (e.g. embryonic and early stages of tissue growth), able to re-grow. Therefore, main role of tissue engineering approaches is fabrication of synthetic tissues as alternative for biological functions during the cells' regeneration [2]. Today, the most materials used in tissue engineering for development of scaffolds are bioactive ceramics, synthetic or natural polymers, and polymer-ceramic composites. Fabrication of nanocomposite materials by organic biopolymers and nanoparticles at molecular level is used for introduction of beneficial materials from natural sources. Novel biodegradable nanocomposite materials have shown good mechanical, structural, economical, and environmental properties [3].

Chitosan (CS) is an abundant natural biopolymer prepared by deacetylation of chitin obtained from the shell of crustaceans and can be transformed to scaffold, fiber, bead, and powder. CS is widely used in pharmaceutical technologies since it exhibits interesting characteristics such as bioadhesion (ability in binding to negatively charged surfaces such as skin and mucosa), wound-healing, and antibacterial activity [4]. Moreover, it is a natural renewable resource by unique properties of biocompatibility, biodegradability and nontoxicity, and can interact with metal ions, dyes, proteins, nucleic acids, lipids, herbicides, pesticides and humic acids. Like other cationic polymers, CS is a cationic polysaccharide by excellent antibacterial activity against various bacteria, viruses and fungi. Importantly, its antibacterial activity depends on molecular weight, degree of deacetylation, temperature, and pH of solution [5].

Polyvinyl alcohol (PVA) is a nontoxic biocompatible biopolymer frequently used as surfactant in different nano-based formulations owing to its significant impact on their mechanical properties [6]. PVA-based composites are served as useful scaffolds with acceptable thermal and chemical stability allowing low protein adsorption for bio-adhesive applications [7]. PVA is added to CS to improve the mechanical strength, biodegradability, and hydrophilic properties of composite membranes [8].

Graphene is a two dimensional monolayer compound, which is formed by arrangement of carbon atoms. It is composed of honeycomb lattice structure with sp2 hybridization. The specific characteristics of graphene including thermal, electronic, mechanical and optical features have made it a suitable candidate for several applications [9]. Graphene and graphene-based nano structures are interested for several biomedical applications including drug delivery, bioimaging, tissue engineering and antimicrobial studies [10-12]. High conductivity and surface area of graphene promotes cell adhesion and proliferation [13]. Graphite oxide is transformed to graphene oxide (GO) by Hummer's technology through which the oxygenated functional groups are rearranged and attached to the edges and the basal plane of individual GO sheets. These changes increase hydrophilicity of GO and help in formation of stable colloidal solution in water with large surface area, which affect its biocompatibility. It leads to wide application in biomedical fields [14]. GO stimulates cell proliferation by dose dependent manner. Antifungal and antibacterial activity of GO has introduced it for wound healing. GO demonstrates the antibacterial activity in different ways such as oxidative stress, membrane stress, and cell wrapping [15]. Inherent chemical structure of GO (amine groups) and CS (epoxy groups) provides cross-linking reactions similar to the curing activity of epoxy resin [16]. If the cross-linking

reactions occur, the enhanced interface is expected in GO cross-linked CS nanocomposites.

Although, there have been several studies on CS-PVA/GO scaffold in the world, less research has been done to examine their chemical and biological properties. In our previous work, physical and mechanical properties of CS-PVA/GO films was studied [17]. The present work was conducted to investigate biological characteristics of CS/PVA polymers reinforced with GO for wound healing.

2. Materials and methods

2-1- Materials

CS (molecular weight of 161,000 g/mol, deacetylation degree of 75.6%, and viscosity of 1406 m.Pas) and PVA (hydrolysis rate of 98- 99% and molecular weight of 31,000–50,000 g/mol) were purchased from Sigma Aldrich (USA). GO (synthesized by Hummer's technique) was bought at concentration of 4 g/l from Tamad Kala (Iran). Acetic acid was prepared from SD Fine Chemical (India).

2-2- Scaffold preparation

The scaffolds were fabricated according to the method described by Pendele et al. [18]. At first, 1 g of CS was mixed with 100 ml of acetic acid (1% v/v) for 20 h at 1100 rpm. Then, 1 g of PVA was dissolved in 100 ml of water at 80 ^{o}C and stirred for 1 h at 1100 rpm. CS gel was mixed with PVA solution and stirred for 2 h at 35 ^{o}C at 1100 rpm. The mixture was poured into a Petri dish and placed in oven at 45 ^{o}C for 30 h. The scaffold was removed from the mold and placed in a vacuum oven for 24 h. To prepare a homogeneous mixture, solutions of GO at different concentrations were subjected to sonication (Bandline, Germany) with power of 75 W under frequency of 20 kHz for 60 min. After GO addition to the polymer solution, the final mixture was stirred with a mechanical mixer for 30 min and sonicated at power of 60 W for 1 h. The CS-PVA (50:50) scaffolds were similarly prepared.

2-3- Characterization

2-3-1- FT-IR spectroscopy

Structure of the nanocomposites was investigated by FT-IR spectra achieved by Bruker Tensor 27 Infrared Spectrometer (Germany) within the wavenumber range of 400-4000 cm^{-1}.

2-3-2- Morphology of nanocomposites

Morphology of complexes was studied by scanning electron microscope (SEM) (model EM 3200 at 30 kV, Iran). Phase of materials and their crystallinity were examined by X-ray diffractometer (Broker XRD machine D8 Advance, Iran) by Cu-K radiation (1.5405 Å) over a range of 5-80 ° angle, step size of 0.02, scan speed of 4 °/min at 30 kV and 40 mA.

2-4- Antibacterial activity assessment

To investigate antimicrobial activity of the scaffolds, *Micrococcus luteus* as a gram positive bacteria and *Pseudomonas aeruginosa* as a gram negative bacteria were used. Amount of 50 µl of the bacterial suspension was cultured on the surface of Mueller-Hinton agar. In the culture medium, four cavities with diameter of 5 mm were created. Small circular pieces of the nanocomposite scaffold (d = 10 mm) were placed on the plates inoculated by the bacteria. The plates were incubated at 37 °C for 24 h and then diameter of clear zone was measured.

2-5- Cell viability assessment

To study biocompatibility, quantitative toxicity and fibroblast cell culture tests were performed on CS-PVA (50:50) samples and nanocomposite scaffold [18]. Quantitative toxicity test was done according to ISO10993-5 using MTT (3-(4,5-dimethylthiazol-2-yl)-2,5-diphenyltetrazolium bromide) and the absorbance was read at 570 nm in a Beckman Counter reader (USA). In fibroblast cell culture test, mouse fibroblast cells (l929) were prepared from Pasteur Institute of Iran. The cells were maintained in RPMI culture medium containing 10% FBS serum under 5% CO_2 and 95% moisture at 37 °C. Cell culture with density of 2.5×10^4 cm^2 was inserted on the polymer

complex and the nanocomposite scaffold containing 3% (w/w) GO. Percentage of the living cells and rate of cell proliferation on the scaffold surface were measured and compared using light microscope after 48 h.

2-6- Statistical analysis

Descriptive data were expressed as mean ±standard deviation. The analysis of data was performed by student t-test with GraphPad Prism 6.0, and Origin Pro 8.0. Differences of data were significant at $p < 0.05$.

3. Results and discussion

3-1- FT-IR spectroscopy

FT-IR spectra of GO, CS-PVA (50:50) and CS-PVA (50:50)/GO 3% (w/w) nanocomposite are shown in Figure 1. For GO, strong –OH peak at 3300 cm^{-1}, C=O at 1717 cm^{-1}, C–O at 1378 cm^{-1}, and C–O–C at 1015 cm^{-1} are clearly visible. A small C=C peak at 1624 cm^{-1} is related to the remaining sp^2 orbital [19]. The CS-PVA (50:50) /GO 3% (w/w) nanocomposite showed a new peak at 1706 cm^{-1} related to carboxyl groups from GO surface which approves presence of GO within the CS-PVA (50:50) polymeric mixture. In general, the indicator transmittance peaks of CS-PVA (50:50)/GO 3% (w/w) nanocomposite scaffold are approximately similar to those of CS-PVA (50:50).

3-2- XRD spectroscopy

Figure 2 indicates XRD patterns of CS, PVA, CS-PVA (50:50), and CS-PVA (50:50)/GO 3% (w/w) nanocomposite scaffolds. With regard to CS, main diffraction peak was observed at 2θ = 20.3°, which presents crystalline structure of CS [20]. PVA showed a distinct diffraction peak at 2θ = 19.31° and a shoulder at 2θ= 22° specific to crystalline PVA [21]. Two characteristic peaks at 2θ = 11.8° and 2θ = 19.4° were observed for CS-PVA (50:50). The CS peak at 2θ = 20.3° disappeared in CS-PVA (50:50), which confirmed good compatibility of CS and PVA. In addition, the indicator peak of PVA at 2θ = 19.31° broadened in CS-PVA (50:50), which referred to intermolecular interactions of CS and PVA. Addition of CS resulted in decreased crystallinity of PVA. Detection of GO characteristic peak in the composite was difficult. Disappearance or weakening of GO peak shows that most of GO were diffused into the polymeric matrix and its peak overlapped with CS peak. As a result, GO is uniformly distributed into CS-PVA (50:50) complex which is of interest for preparation of nanocomposite films with improved properties.

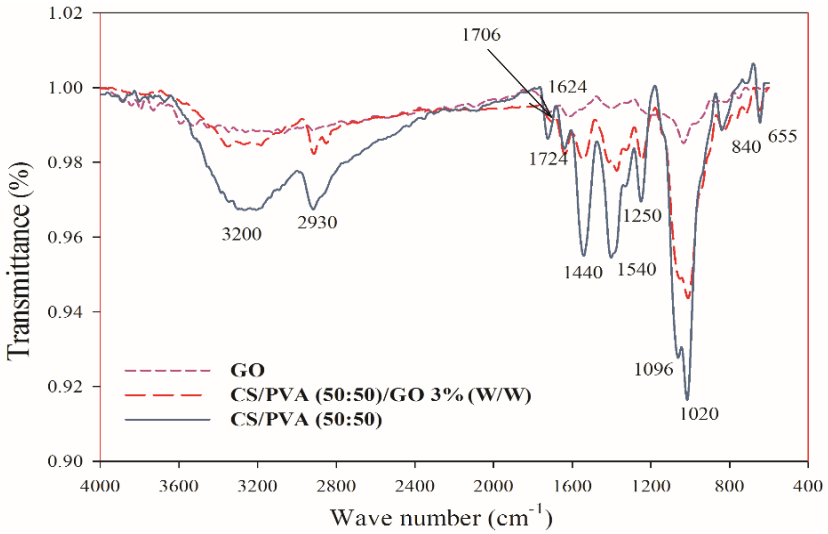

Figure 1- FT-IR spectra of GO, CS-PVA (50:50), and CS-PVA (50:50)/GO 3% (w/w) nanocomposite scaffold

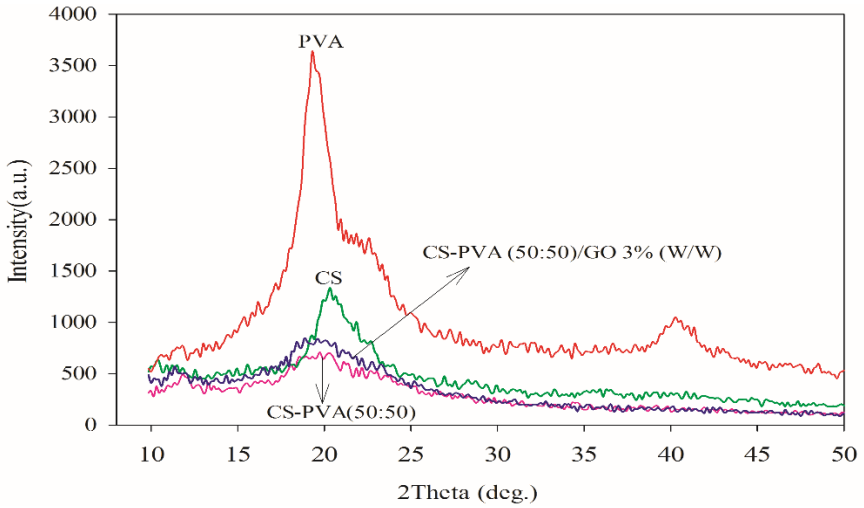

Figure 2- XRD pattern of PVA, CS, CS-PVA (50:50), and CS-PVA (50:50)/GO 3% (w/w) scaffold

3-3- Morphology studies

As shown in Figure 3, surface roughness of the scaffolds increased by increasing the GO concentration in the complex. In this regard, morphology of the scaffolds changed from smooth (Figure 3a) to rough structure (Figures 3b and 3c) [18]. In agreement, another study reported that surface of pure CS-PVA scaffold is smooth, continuous and compact [22]. It is due to PVA good compatibility with polysaccharides such as CS. In fact, when GO added to the polymer composite, the surface roughness and cavities increase followed by improved adhesion and survival rate of cells compared to the raw sample. In general, the interconnected pores provide a suitable culture medium to develop cell adhesion, tissue proliferation and growth, and adequate nutrient flow into the cell [23] that are important in scaffold fabrication studies. Interestingly, GO can significantly reduce the oxidative stress and weakness in cells [24].

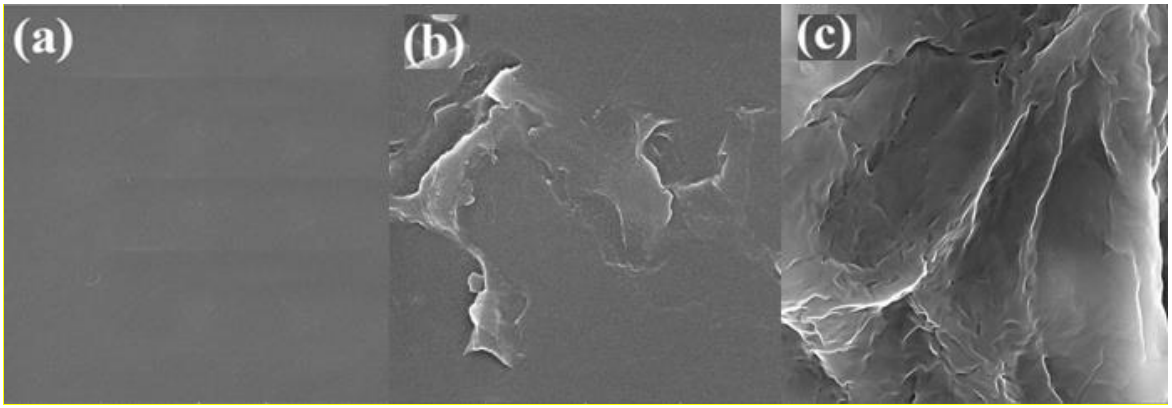

Figure 3- SEM images of (a) CS-PVA (50:50), (b) CS-PVA (50:50)/GO 1% (w/w) nanocomposite scaffolds, (c) CS-PVA (50:50)/GO 3% (w/w) nanocomposite scaffolds

3-4- Antibacterial activity assay

Antibacterial activity of the polymeric blend and nanocomposites scaffold containing different concentrations of GO were investigated against gram-positive bacteria of *Micrococcus luteus* and gram-negative bacteria of *Pseudomonas aeruginosa*. The results of inhibition diameter are shown in Figures 4 and 5. Antimicrobial impact was observed by the polymers' complex due to the inhibitory effect of CS driven by its cationic

groups. Interaction of positively charged CS with negatively charged endotoxins of gram-negative bacteria reduces their acute toxicity [25].

Inhibition activity of the nanocomposite scaffold containing 3% w/w GO was higher than the other nanocomposite scaffolds. With regard, Liu et al. showed that antibacterial activity of GO depends on its concentration. In addition, they believed that its surface structure significantly affect the antimicrobial properties [26].

Structure of GO is chemically modified by hydroxyl, epoxy, and carboxyl groups, which lead to its improved dispersion in polymer matrices followed by severe antibacterial activity with low cell toxicity. Antibacterial activity of GO is also driven by its oxidative role in peroxidation of lipids [27]. *Pseudomonas aeruginosa* loses its cellular integrity in the presence of GO as a result of cell membrane damage and release of cytoplasm into the environment. In fact, such irreversible cell destruction of the bacterium is facilitated by both oxidative stress and damage to the cell membrane by the sharp edges of GO sheets. Therefore, GO can penetrate into the cell membrane and physically disturb its integrity [27, 28].

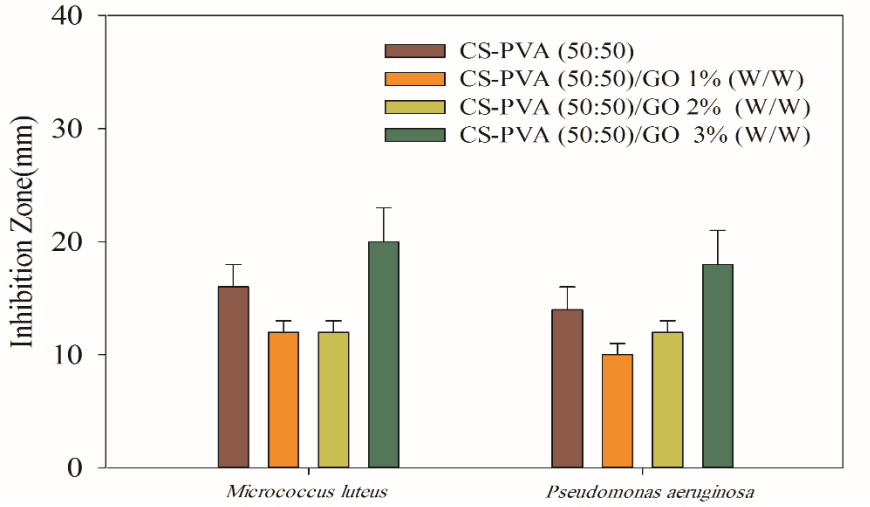

Figure 4- Inhibition diameter of CS-PVA (50:50) and nanocomposite scaffolds containing different concentrations of GO against *Micrococcus luteus* and *Pseudomonas aeruginosa*

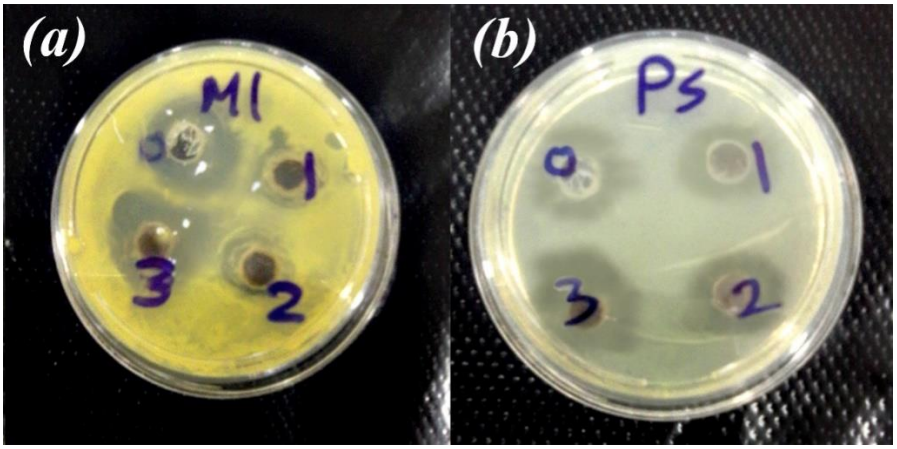

Figure 5- Inhibition zones of CS-PVA (50:50) and nanocomposite scaffolds containing different concentrations of GO against (a) *Micrococcus luteus* and (b) *Pseudomonas aeruginosa*. The numbers 0, 1, 2, and 3 refer to CS-PVA (50:50), CS-PVA (50:50)/1% w/w GO, CS-PVA (50:50)/2% w/w GO, and CS-PVA (50:50)/3% w/w GO scaffolds, respectively.

3-5- Morphology and biocompatibility assay

Figure 6 shows SEM images of fibroblasts L929 cells cultured onto CS-PVA (50:50) and CS-PVA (50:50)/3% w/w GO scaffolds after cell seeding for 48 h. It is observed that shape of the nanocomposite scaffold was well retained after soaking in the culture medium for 48 h, and the cells spread appropriately into the structures. The cells growing on CS-PVA (50:50) appeared in spindle shape (Figure 6a) while those on the nanocomposite scaffolds showed polygonal and stretchy shape (Figure 6b) and tended to form colony or aggregate. These differences were possibly due to the characteristics of the scaffold surface. When GO is added to CS-PVA (50:50), roughness and surface cavities on the nanocomposites increase. Then, adhesion of cells and their survival will increase compared to the polymers alone which affect their metabolic activity. In addition, incorporation of GO to the polymers remarkably improves the cellular response and significantly promotes the cells' growth.

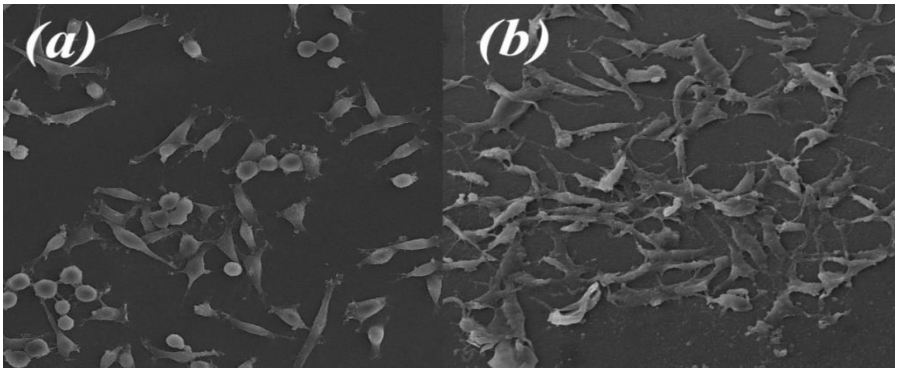

Figure 6- Morphology of the cells after seeding for 48 h: (a) the cells exposed to CS-PVA (50:50), (b) the cells exposed to nanocomposite scaffolds containing 3% w/w GO

MTT assay was further conducted to quantify proliferation of L929 cells cultured onto CS-PVA (50:50) and CS-PVA (50:50)/3% w/w GO scaffolds within 48 h (Figure7). It is observed that the cells on the nanocomposite scaffolds proliferated faster than those on CS-PVA (50:50), mainly due to GO nano-sheets that facilitated the cells' proliferation. Presence of GO into CS-PVA (50:50) could improve viability of the cells through which the viability increased to 84% compared to CS-PVA (50:50). This result was consistent with SEM graphs. The improved cellular response in the presence of GO nano-sheets was related to protein adsorption from the culture media onto the GO rough structure, which significantly promoted the cells' growth and proliferation.

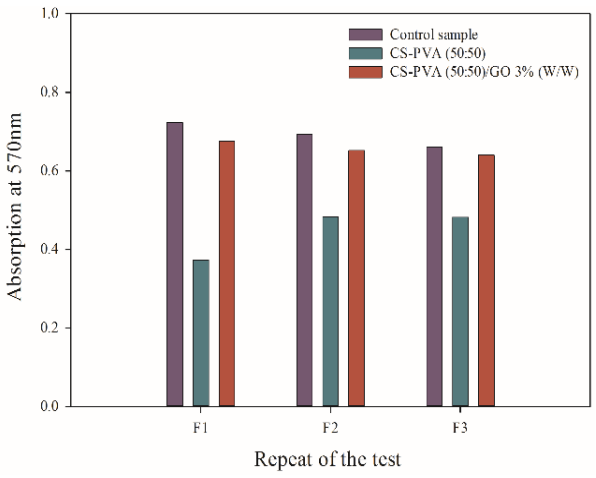

Figure 7- Results of MTT test for CS-PVA (50:50) and nanocomposite scaffolds containing 3% w/w GO in three replications

4- Conclusion

Nanocomposite scaffolds reinforced with GO nano-sheets at different concentrations (1, 2 and 3% w/w) were successfully prepared. SEM graphs confirmed that GO nano-sheets were uniformly dispersed in the matrix, as the surface roughness was increased by increasing the concentration of GO. Importantly, CS-PVA (50:50) scaffold showed a continuous and homogeneous phase and no evidence of phase separation was observed. It might be related to compatibility of the polymers and surface smoothness of the complex. The nanocomposite scaffold containing 3% w/w GO showed higher antibacterial activity than the other treatments. Moreover, our *in vitro* experiment confirmed its ability in wound healing. In further studies, we will examine other polymeric systems doped with GO for rapid wound healing *in vitro* and *in vivo*.

5- Acknowledgement

Authors thank the Department of Pharmacology, School of Medicine, Cellular and Molecular Research Center, Guilan University of Medical Sciences.

References

1. Doostmohammadi A, Esmaeili F, Nikbakht Katouli S. Fabrication of chitosan/poly (vinyl alcohol)/carbon nanotube/bioactive glass nanocomposite scaffolds for neural tissue engineering. Journal of Nanomedicine Research. 2016; 4(3): 1-8. https://doi.org/10.15406/jnmr.2016.04.00088

2. Habibi S, Razaghpour M, Allah Gholi Ghasri MR, Nazokdast H. Properties and medical applications of electrospun chitosan nanofibers: a review. Journal of Textile Science and Technology. 2014. 4(1): 43-55. In Persian.

3. Ray SS, Okamoto M. Biodegradable polylactide and its nanocomposites: opening a new dimension for plastics and composites. Macromolecular Rapid Communications. 2003; 24(14): 815-840. https://doi.org/10.1002/marc.200300008

4. Yuste J, Quetglas E, Azanza J. The most common infections in the transplanted patient. An Sist Sanit Navar. 2006: 175-205.

5. Yuvaraja G, Pathak JL, Weijiang Z, Yaping Z, Jiao X. Antibacterial and wound healing properties of chitosan/poly (vinyl alcohol)/zinc oxide beads (CS/PVA/ZnO). International Journal of Biological Macromolecules. 2017; 103: 234-241. https://doi.org/10.1016/j.ijbiomac.2017.05.020

6. Itoh H, Li Y, Chan KHK, Kotaki M. Morphology and mechanical properties of PVA nanofibers spun by free surface electrospinning. Polymer Bulletin. 2016; 73(10): 2761-2777.

7. Wang W, Zhang L, Pan Y, Lhamo T, Zhang C, Li B. The complete mitochondrial genome of the *Schizothorax curilabiatus* (Cypriniformes: Cyprinidae). Mitochondrial DNA Part B. 2017; 2(2): 683-684. https://doi.org/10.1080/23802359.2017.1383202

8. Ahmed R, Tariq M, Ali I, Asghar R, Khanam PN, Augustine R, et al. Novel electrospun chitosan/polyvinyl alcohol/zinc oxide nanofibrous mats with antibacterial and antioxidant properties for diabetic wound healing. International Journal of Biological Macromolecules. 2018; 120: 385-393. https://doi.org/10.1016/j.ijbiomac.2018.08.057

9. Zhu Y, Murali S, Cai W, Li X, Suk JW, Potts JR, et al. Graphene and graphene oxide: synthesis, properties, and applications. Advanced Materials. 2010; 22(35): 3906-3924. https://doi.org/10.1002/adma.201001068

10. Goenka S, Sant V, Sant S. Graphene-based nanomaterials for drug delivery and tissue engineering. Journal of Controlled Release. 2014; 173: 75-88. https://doi.org/10.1016/j.jconrel.2013.10.017

11. Imani R, Mohabatpour F, Mostafavi F. Graphene-based nano-carrier modifications for gene delivery applications. Carbon. 2018; 140: 569-591. https://doi.org/10.1016/j.carbon.2018.09.019

12. Prakash J, Venkatesan M, Prakash JS, Bharath G, Anwer S, Veluswamy P, et al. Investigations on the in-vivo toxicity analysis of reduced graphene oxide/TiO_2 nanocomposite in zebrafish embryo and larvae (*Danio rerio*). Applied Surface Science. 2019; 481: 1360-1369. https://doi.org/10.1016/j.apsusc.2019.03.287

13. Liang Y, Zhao X, Hu T, Chen B, Yin Z, Ma PX, et al. Adhesive hemostatic conducting injectable composite hydrogels with sustained drug release and photothermal antibacterial activity to promote full-thickness skin regeneration during wound healing. Nano Micro Small. 2019; 15(12): 1-17. https://doi.org/10.1002/smll.201900046

14. Mitra T, Manna PJ, Raja STK, Gnanamani A, Kundu PP. Curcumin loaded nano graphene oxide reinforced fish scale collagen–a 3D scaffold biomaterial for wound healing applications. RSC Advances. 2015; 5(119): 98653-98665. https://doi.org/10.1039/C5RA15726A

15. Khan MS, Abdelhamid HN, Wu HF. Near infrared (NIR) laser mediated surface activation of graphene oxide nanoflakes for efficient antibacterial, antifungal and wound healing treatment. Colloids and Surfaces B: Biointerfaces. 2015; 127: 281-291. https://doi.org/10.1016/j.colsurfb.2014.12.049

16. Meng F, Zheng S, Li H, Liang Q, Liu T. Formation of ordered nanostructures in epoxy thermosets: a mechanism of reaction-induced microphase separation. Macromolecules. 2006; 39(15): 5072-5080. https://doi.org/10.1021/ma060004

17. Saeedi F, Montazeri A, Bahari Y, Pishvaei M, Jannat B. A study on the viscoelastic behavior of chitosan-polyvinyl alcohol-graphene oxide nanocomposite films as a wound dressing. Polymers and Polymer Composites. 2020: 1-14. https://doi.org/10.1177/0967391120962375

18. Pandele AM, Ionita M, Crica L, Dinescu S, Costache M, Iovu H. Synthesis, characterization, and in vitro studies of graphene oxide/chitosan–polyvinyl alcohol films. Carbohydrate Polymers. 2014; 102: 813-820. https://doi.org/10.1016/j.carbpol.2013.10.085

19. Zhang W, Zhou C, Lei A, Zhang Q, Wan Q, Zou B. Fast and considerable adsorption of methylene blue dye onto graphene oxide. Bulletin of Environmental Contamination and Toxicology. 2011; 87(1): 86-90. https://doi.org/10.1007/s00128-011-0304-1

20. Kisku SK, Swain SK. Synthesis and characterization of chitosan/boron nitride composites. Journal of the American Ceramic Society. 2012; 95(9): 2753-2757. https://doi.org/10.1111/j.1551-2916.2012.05140.x

21. Ricciardi R. Auriemma F, De Rosa C, Laupretre F. X-ray diffraction analysis of poly (vinyl alcohol) hydrogels, obtained by freezing and thawing techniques. Macromolecules. 2004; 37(5): 1921-1927. https://doi.org/10.1021/ma035663q

22. Ma Q, Liang T, Cao L, Wang L. Intelligent poly (vinyl alcohol)-chitosan nanoparticles-mulberry extracts films capable of monitoring pH variations. International Journal of Biological Macromolecules. 2018; 108: 576-584. https://doi.org/10.1016/j.ijbiomac.2017.12.049

23. Dubey P, Gopinath P. PEGylated graphene oxide-based nanocomposite-grafted chitosan/polyvinyl alcohol nanofiber as an advanced antibacterial wound dressing. RSC Advances. 2016; 6(73): 69103-69116. https://doi.org/10.1039/C6RA12192F

24. Khorsand Zak A. Synthesis and characterization of rGO-ZnO nanocomposites and investigating their potential for medical applications. Journal of Research on Many-body Systems. 2017; 7(13): 61-70. https://doi.org/10.22055/jrmbs.2017.13014

25. Grande-Tovar CD, Serio A, Delgado-Ospina J, Paparella A, Rossi C, Chaves-Lopez C. Chitosan films incorporated with *Thymus capitatus* essential oil: mechanical properties and antimicrobial activity against degradative bacterial species isolated from tuna (*Thunnus* sp.) and swordfish (*Xiphias gladius*). Journal of Food Science and Technology. 2018; 55(10): 4256-4265. https://doi.org/10.1007/s13197-018-3364-y

26. Liu S, Zeng TH, Hofmann M, Burcombe E, Wei J, Jiang R, et al. Antibacterial activity of graphite, graphite oxide, graphene oxide, and reduced graphene oxide: membrane and oxidative stress. ACS Nano. 2011; 5(9): 6971-6980. https://doi.org/10.1021/nn202451x

27. Fan J, Grande CD, Rodrigues DF. Biodegradation of graphene oxide-polymer nanocomposite films in wastewater. Environmental Science: Nano. 2017; 4(9): 1808-1816. https://doi.org/10.1039/C7EN00396J

28. Perreault F, de Faria AF, Nejati S, Elimelech M. Antimicrobial properties of graphene oxide nanosheets: why size matters. ACS Nano. 2015; 9(7): 7226-7236. https://doi.org/10.1021/acsnano.5b02067